Vol. 10: 115–125, 1998 | CLIMATE RESEARCH Clim Res | Published August 14

The Gulf of Mexico mid-tropospheric response to El Niño and La Niña forcing

Anthony J. Vega[1,*], Robert V. Rohli[2], Keith G. Henderson[3]

[1]Department of Anthropology, Geography and Earth Science, Clarion University of Pennsylvania, Clarion, Pennsylvania 16214, USA

[2]Department of Geography, Kent State University, Kent, Ohio 44242, USA

[3]Department of Geography and Anthropology, Louisiana State University, Baton Rouge, Louisiana 70803, USA

ABSTRACT: This analysis further refines Ropelewski & Halpert's (1987; Mon Wea Rev 115:1606–1626) analysis which investigates the relationship between El Niño-La Niña/Southern Oscillation events and southern United States precipitation. Comparisons are made between eigenvector-derived mid-tropospheric (500 mb) flow patterns over North America during extreme El Niño and La Niña months and a base climatology. In addition, the patterns are correlated to regional precipitation anomalies for the southern United States to determine mean surface responses. Cool season (November to March) months are divided into all winter months (AWM), positive anomaly months (PAM), and negative anomaly months (NAM). The extreme anomaly months were determined as any month with a Southern Oscillation Index (SOI) ± 1 standard deviation from the standardized mean. Therefore, the PAM and NAM anomalies represent the La Niña and El Niño extreme phases of the SOI, respectively. Results suggest that the positive (La Niña) SOI phase elicits a greater surface precipitation response than the El Niño phase. This is caused by substantial changes in the primary longwave flow during opposite SOI phases. During AWMs and NAMs, similar flow patterns, dominated by the Pacific/North American (PNA) teleconnection, prevail which induce similar regional precipitation responses. During PAMs, the mid-tropospheric flow shifts to a hybrid flow pattern which is between the PNA and the Tropical Northern Hemisphere teleconnections. Such displacement in the longwave flow variation centers ultimately affects jet stream flow and precipitation forcing, resulting in negative precipitation anomalies across the southern United States.

KEY WORDS: El Niño · La Niña · Precipitation · Climatology · Gulf of Mexico

1. INTRODUCTION

Relationships between El Niño and the United States climate have been well documented. In particular, southern U.S. precipitation has been shown to be strongly tied to El Niño. Douglas & Englehart (1981) found a strong relationship between El Niño events and Florida precipitation while Ropelewski & Halpert (1987) described a precipitation response to El Niño forcing for the southeastern U.S. Henderson & Vega (1996) highlighted a cool season precipitation response to El Niño events in the western and central Gulf Coast states while Vega et al. (1997) defined an annual El Niño-induced precipitation signal in the central Gulf South. The predominant mechanism used to explain these relationships focuses on increased energy and moisture fluxes from the tropics to the mid-latitudes during El Niño events. The result is a highly amplified mean mid-latitude atmospheric flow regime over the U.S. The increase in the meridional component of the jet relates to more frequent cool season cyclogenesis in the western Gulf of Mexico (Manty 1993). While much has been done to understand the initial formation of these singular storm events and their initial relationship to southeastern U.S. precipitation, little climatological work has been done to determine the general mid-tropospheric response to both El Niño and La Niña (opposite extreme) forcing over the Gulf of Mexico cyclogenetic region.

*E-mail: avega@clarion.edu

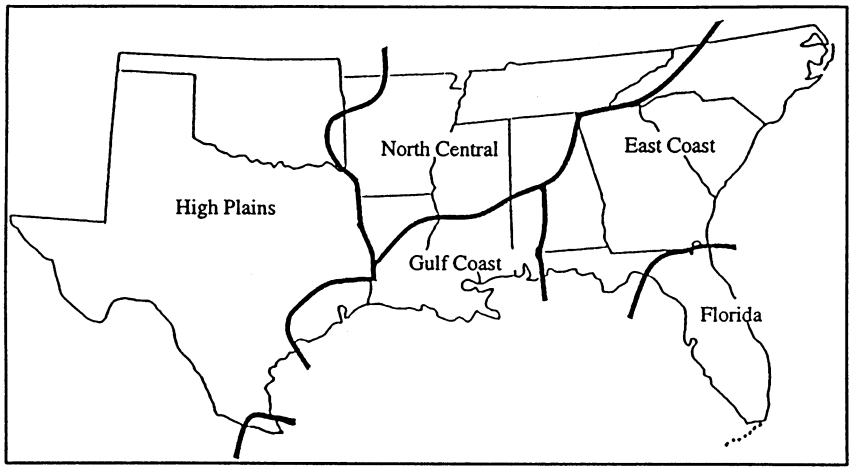

Fig. 1. Winter precipitation regions for the southern United States (Henderson & Vega 1996)

This analysis defines the surface precipitation response over an 11-state region comprising the southern United States (Fig. 1), updating Ropelewski & Halpert's (1987) work. In addition, the analysis examines the primary mid-tropospheric flow patterns during the cool season as well as those during anomalously strong El Niño and La Niña months to determine the regional atmospheric response to Southern Oscillation forcing. These differences in regional flow provide a greater understanding of the forcing mechanisms for anomalous El Niño-La Niña/Southern Oscillation (ENSO)-induced atmospheric conditions over the southeastern U.S., perhaps with forecasting applications.

2. LITERATURE REVIEW

2.1. Effects of ENSO

Many studies have correlated El Niño events with mid-latitude atmospheric phenomena (e.g. Trenberth 1976, Douglas & Englehart 1981, Rasmusson & Carpenter 1982, Bradley et al. 1987). Ropelewski & Halpert (1987) identified precipitation links between major land masses and El Niño. Direct correlations were found for the major land masses in the Southern Hemisphere, but El Niño-enhanced precipitation in the Northern Hemisphere was less evident. They did, however, find that El Niño is related to enhanced winter precipitation in the southeastern United States, though the processes which link El Niño to the precipitation anomalies were not examined in detail. The authors state that 'in the subtropics and higher latitudes there are suggestions of El Niño-related precipitation in India, Australia, sections of Mexico and the United States'. Within these areas the enhanced precipitation is the result of processes which link El Niño and tropical circulation to the subtropics and mid-latitudes (Conrad 1941, Nicholls 1988). The equatorial ocean is responsible for anomalously great sources of heat which maintain an anomalous flux of momentum to the mid-latitude westerlies (Bjerknes 1969). This response to large-scale thermodynamic forcing may account for a considerable degree of precipitation variability for a place or region.

Other studies have concentrated on the effects of El Niño events on the southeastern U.S. For example, Angel & Korshover (1987) found significant increases in annual-average cloudiness in the south-central United States during El Niño years. Greater moisture advection into the southern U.S., especially during autumn, has been correlated to the El Niño phenomenon (Vega et al. 1997). Henderson & Vega (1996) found a corresponding significant increase in autumn precipitation in the southern U.S. during El Niño events. Wet winters in southern Florida have been statistically linked to warm water events along the equator in the central Pacific while dry conditions have been associated with cold water events (La Niña) (Douglas & Englehart 1981). In addition, anomalously cold winters in the southeastern U.S., characterized by persistent 700 mb flow anomalies, are correlated to the El Niño phenomena (Dickson & Namias 1976). Arkin et al. (1980) show similar patterns in the southern U.S. for years with a low Southern Oscillation Index (SOI).

Although these studies and many others identify correlations, the processes by which ENSO affects particular areas are not examined in detail. Links between mid-latitude forcing and El Niño events are evident in the anomalous deep winter Aleutian Low and in the 700 mb geopotential heights during El Niño years. The patterns are related to the Pacific/North American (PNA) teleconnection (Wallace & Gutzler 1981), particularly the highly amplified positive PNA pattern (Leathers et al. 1991). Resulting meridional jet flow

increases wintertime cyclogenesis in the Gulf of Mexico with the advent of a well-developed low-latitude flow regime across northern Mexico and the southern U.S. (Douglas & Englehart 1981, Hsu 1993, Manty 1993). The mid-latitude response is triggered by enhanced Hadley circulation which results from a weakening of the Walker circulation during El Niño events. The jet flow is caused by a strengthened Pacific Subtropical High (STH), which is enhanced through the anomalously strong Hadley circulation during these times. The transport of energy and mass occurs through this circulation primarily during the winter season when the circumpolar vortex expands and allows net transport away from the tropics (Philander 1990). Consequently, cyclogenesis is usually enhanced by upper-level venting (speed divergence) caused by a low-latitude mean jet, especially over the northwestern Gulf where moist unstable air is located along the continental shelf break in association with large sea surface temperature (SST) gradients (Lewis & Hsu 1992).

Below-normal height fields over the Gulf suggest invasions of polar fronts into the region and subsequent cyclogenesis in association with the low-latitude split flow. Gulf cyclogenesis is typically associated with a southward displacement of the upper-tropospheric westerly flow and mean subtropical jet position. Wet winters in the southern U.S. are therefore typically preceded by heavy rainfall events in the central equatorial Pacific during autumn. This flow is followed by enhanced low-latitude advection across North America and increased frontal activity in the Gulf of Mexico. Thus, mean advection typically increases across the Northern Pacific, Gulf of Mexico, and Western Atlantic Ocean.

2.2. Gulf cyclogenesis

Cool season Gulf of Mexico cyclogenesis is supported by the extreme negative phase of the SOI (El Niño) when the mid-latitude westerlies are supplied with tremendous amounts of energy and moisture (Philander 1990, Hsu 1993). Conversely, during La Niña events, cyclogenesis is suppressed due to a reduced energy and moisture flux (Manty 1993). Increased Gulf cyclogenesis during El Niño events has been related to spin-off eddies in the Gulf of Mexico loop current (Walker 1993). The warm water loop current, and/or the spin-off eddies, typically couples with an enhanced upper-level jet in rapid cyclogenetic events (Lewis & Hsu 1992). The jet provides upper-level venting over an enhanced cool season baroclinic zone set up by the warm water eddies. These eddies typically reside for long periods adjacent to the shelf-break near the Texas coast (Walker 1993). When positive vorticity advection and speed divergence present in the upper atmosphere couple with a strong SST front located off the shelf-break and the resultant low-level instability, a high frequency of cyclones is possible, some of which become meteorological 'bombs' (Sanders & Gyakum 1980, MacDonald & Reiter 1988).

Although these mechanisms are fairly well understood in hindsight, little is known about the mechanisms which determine when anomalous cyclogenesis (both frequency and intensity) will take place. During La Niña years, the same antecedent conditions may be present but cyclogenesis typically does not achieve the frequency and/or intensity of that during El Niño years. For this reason it is important to examine and compare the climatology of mid-tropospheric characteristics during anomalously strong El Niño and La Niña months to determine differences in the primary atmospheric patterns found during these times. Also, little has been done to determine how the mid-troposphere changes between these extreme SOI times as opposed to the 'normal' cool season climatology.

3. DATA AND METHODS

In order to define primary modes of mid-tropospheric (500 mb) height variation important to the United States surface climate, all cool season (November to March) gridded 500 mb geopotential heights were extracted from the NMC (National Meteorological Center) grid (NCAR 1993) for the time period 1946 to 1991. This data set includes monthly mean geopotential heights based on twice-daily (00:00 and 12:00 h UTC) observations for 1977 equally spaced grid points throughout the Northern Hemisphere. It must be noted that a change of observation time occurred during the International Geophysical Year of 1957; however, examination of the corresponding time-series revealed no appreciable data discontinuities. The spatial domain used in this analysis includes all grid points between 20–60°N and 70–140°W. The defined domain was chosen to capture atmospheric variability over the continental United States and surrounding ocean environments, especially those upstream of the study area.

Primary modes of atmospheric variability capturing the majority of temporal and spatial variation were found through an unrotated Principal Components Analysis (PCA) (Dunteman 1989). The unrotated solutions were chosen over a rotated PCA because the analysis represents a synoptic-type classification. Rotated solutions are inappropriate for this type of classification as the unrotated solutions are the most parsimonious and yield the maximal amount of data variance (Yarnal 1993).

Incorporation of the eigenvector methodology for this type of analysis induces a potential limitation in that the number of observations (months) is exceeded by the number of variables (grid points). However, comparisons, both spatial and temporal, to known atmospheric teleconnections suggest that the derived patterns are stable and the potential limitation negligible. The derived modes of variation establish a baseline climatology of mid-tropospheric heights and are referred to hereafter as AWM (All Winter Months). Throughout the analysis, retained PCs were chosen based on scree plot analysis of the corresponding eigenvalues (Appendix 1a). All PCs to the left of a significant break in the eigenvalue slope were retained and further investigated.

The second part of the analysis determines the primary modes of mid-tropospheric variation over the conterminous United States during extreme phases of the SOI. Cool season months are divided into positive (PAM) and negative (NAM) anomaly months. An anomaly month is defined as any month with a monthly SOI of ±1 standard deviation from the monthly standardized mean. All PAMs and NAMs are listed in Table 1. Primary modes of atmospheric variation are found independently for all PAMs and NAMs using PCA and the retention methodology outlined previously (Appendix 1b, c). Simple linear trends were sought in the corresponding component scores (time-series) through linear regression. Such testing indicates whether significant temporal changes occur in component strength. Individual AWM, PAM, and NAM components were independently tested for trend. In addition, comparisons are made between similar PAM and NAM height patterns as reflected through the PCA loadings patterns. Such comparisons highlight similarities and, more importantly, differences between opposite SOI height patterns as they apply to the surface environment. Further comparisons are made between these months and the derived AWM patterns to determine important SOI-related deviations from the base climatology. Correlations determine the importance of the 3 height field groupings to regional precipitation anomalies in the southern U.S.

Table 1. November to March PAMs (La Niña) and NAMs (El Niño), based on SOI values, 1946 to 1993

Extreme negative year/month, n = 28	Extreme positive year/month, n = 43
1952/12, 1957/11, 1958/1, 1961/3, 1963/12, 1965/11, 1966/1, 1966/3, 1969/1, 1972/12, 1977/11, 1977/12, 1978/2, 1981/3, 1982/11, 1982/12, 1983/1, 1983/2, 1983/3, 1986/2, 1986/11, 1986/12, 1987/2, 1987/3, 1990/2, 1990/3, 1991/3, 1991/12	1947/3, 1950/2, 1950/3, 1950/12, 1951/1, 1951/2, 1954/12, 1955/2, 1955/12, 1956/1, 1956/2, 1956/3, 1959/3, 1961/2, 1961/11, 1961/12, 1962/1, 1963/1, 1963/2, 1967/1, 1967/2, 1968/2, 1970/11, 1970/12, 1971/2, 1971/3, 1972/2, 1973/12, 1974/1, 1974/2, 1974/3, 1975/2, 1975/3, 1975/12, 1976/1, 1979/2, 1976/3, 1977/2, 1979/2, 1982/1, 1988/11, 1988/12, 1989/1

4. ANALYSIS

4.1. Precipitation relationships to the SOI

Fig. 1 details winter (DJF) precipitation regions for the southern United States as defined by Henderson & Vega (1996). The regions were found through varimax-rotated PCA of monthly climate division precipitation anomalies for the time period 1946 to 1988. The regional time-series were composed of actual climate division anomalies calculated for each region though the clustering of all related climate divisions. The anomalies were grouped by year and averaged for the winter season (DJF). For this analysis, 2 additional months (November and March) and 3 additional years (1989 to 1991) of precipitation anomalies were added and new regional time-series calculated in order to match the temporal array of the geopotential height analysis.

Table 2 depicts the wintertime correlations of each precipitation region to the standardized SOI. The strong correlation ($\alpha \leq 0.05$) with Florida approximates that found by Douglas & Englehart (1981). Weaker but significant correlations exist between the SOI and the Gulf Coast and High Plains regions, indicating clear relationships between the SOI and precipitation in the southern U.S. Excluding the Florida peninsula, SOI forcing mainly affects the central to western portions of the study region, supporting the hypothesis that phases of the SOI force variations in western Gulf of Mexico cyclogenesis and the resulting storm tracks as

Table 2. Correlations between the SOI and southern United States precipitation regions. EC: East Coast; FL: Florida; GC: Gulf Coast; HP: High Plains; NC: North Central. (Taken from Henderson & Vega 1996.) Significance ($\alpha = 0.10$) indicated in bold

	EC	FL	GC	HP	NC
r	−0.174	−0.700	−0.292	−0.326	0.078
p	0.258	**0.000**	**0.054**	**0.030**	0.611

defined by Manty (1993). The following sections explore relationships between surface precipitation and the 3 mid-tropospheric height field groups.

4.2. Geopotential height analysis

To compare modes of atmospheric flow during all extreme El Niño and La Nina months, 500 mb height anomaly composites were constructed (Fig. 2). The NAM composite indicates lower heights over the Gulf of Mexico while the PAM anomaly composite indicates higher heights over the Gulf of Mexico. From this it is evident that major differences occur between the NAM and PAM groupings. To better determine these differences, forcing associated with each, and the influence on the precipitation regimes of the southern U.S., the heights were subjected to PCA.

4.2.1. All Winter Months

The spatial configuration of the 5 primary AWM geopotential height patterns found through PCA are depicted in Fig. 3. The patterns collectively explain

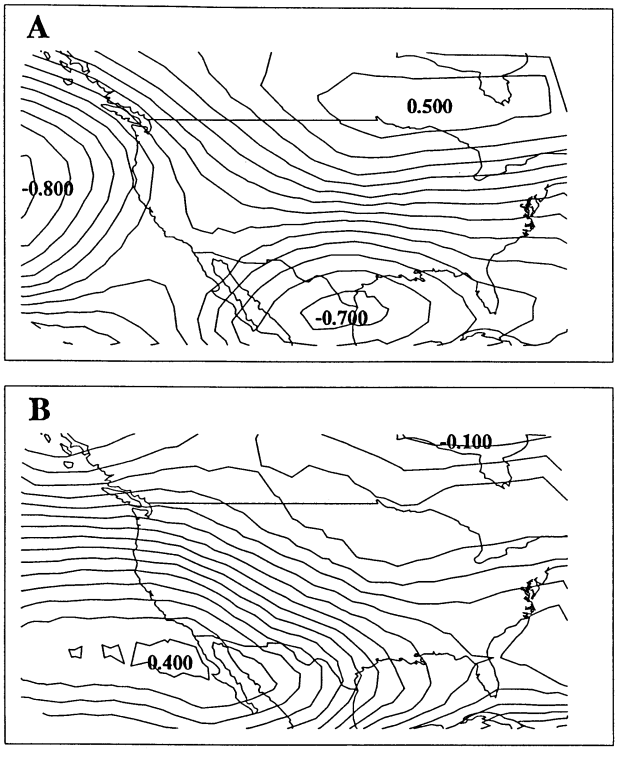

Fig. 2. Wintertime Negative Anomaly Month (NAM, top) and Positive Anomaly Month (PAM, bottom) 500 mb geopotential height anomaly composites

Table 3. Correlations between AWM PCs and southern United States precipitation regions (abbreviations as in Table 2). Significance ($\alpha = 0.10$) indicated in bold

		PC1	PC2	PC3	PC4	PC5
EC	r	−0.1888	−0.1565	−0.0596	−0.0033	0.5486
	p	0.2197	0.3103	0.7006	0.9832	**0.0001**
FL	r	−0.5254	0.3363	−0.3243	0.0266	0.1376
	p	**0.0003**	**0.0269**	**0.0317**	0.8637	0.3731
GC	r	−0.2043	−0.2219	−0.3039	0.0222	0.1936
	p	0.1833	0.1477	**0.0449**	0.8864	0.2079
HP	r	−0.0429	−0.1559	−0.0864	0.3921	0.0401
	p	0.7821	0.3124	0.5769	**0.0085**	0.7962
NC	r	0.1763	−0.5168	−0.0770	−0.0740	0.2280
	p	0.2522	**0.0003**	0.6195	0.6331	0.1366

85.8% of the variance present in the 500 mb geopotential height field. In an unrotated PCA an inherent problem exists with regard to domain shape dependence (Buell 1975); however, a classic 'Buell Sequence' is not readily apparent in this analysis, which lends confidence to the derived patterns. All 5 patterns prove to be related to precipitation in at least one precipitation region as is evident by the significant ($\alpha = 0.05$) correlations portrayed in Table 3. The strongest correlations occur between PC1 and Florida precipitation, PC2 and North Central precipitation, and PC5 and East Coast precipitation, explaining approximately 28, 27 and 30% of the explained precipitation variance, respectively. Two of the components, PCs 2 and 3, relate to multiple regions. Overall, the patterns indicate that lowered heights near or upstream of the related precipitation regions relate to positive precipitation anomalies in that region.

Most of the PC loadings patterns qualitatively approximate known cool season atmospheric teleconnections; however, the first AWM principal component (PC1) does not. The loadings pattern depicts a large action center node over the entire Gulf South (Fig. 3) which in the positive component phase is indicative of high heights along a southwest to northeast transect culminating in a variation action center over Texas. The associated PC scores correlate inversely to Florida precipitation, indicating that high (low) 500 mb heights over Texas and the southeastern U.S. induces negative (positive) precipitation anomalies in the Florida peninsula (Table 3).

PC2 (Fig. 3) is clearly a representation of the PNA teleconnection as the loadings indicate 3 variability action nodes located over the Gulf of Alaska, the Cordillera of western North America, and the southeastern United States. Like signs are shared by the western and eastern action nodes while the middle node is opposite in phase. There is a clear relationship between the pattern and southern U.S. precipitation as

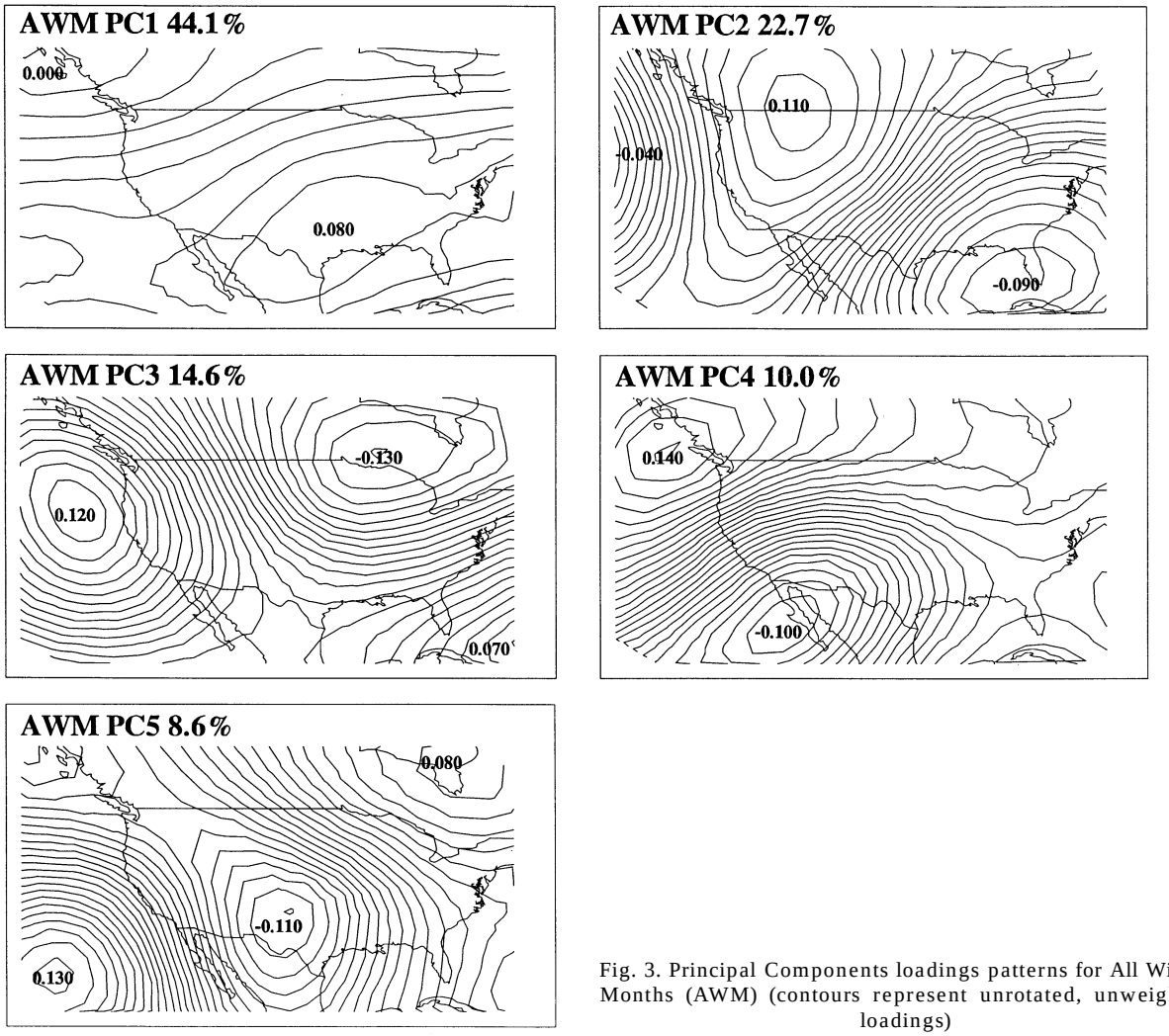

Fig. 3. Principal Components loadings patterns for All Winter Months (AWM) (contours represent unrotated, unweighted loadings)

the PC scores correlate positively to Florida and negatively to North Central precipitation anomalies (Table 3). The positive component mode indicates lower tropospheric heights and cooling over Florida, a characteristic conducive to precipitation forcing (Yarnal & Leathers 1988, Leathers et al. 1991). Higher heights to the west correspond to reduced precipitation in the North Central region.

The loadings pattern of PC3 (Fig. 3) indicates out-of-phase dual action centers over the eastern North Pacific and eastern Canada near Hudson Bay. A third node, in-phase with the eastern Pacific node, is located over the Bahamas. The pattern approximates the Tropical Northern Hemisphere (TNH) teleconnection identified by Mo & Livezey (1986) and further defined by Barnston & Livezey (1987). The pattern is a variation of the PNA except that the action centers are displaced to the east. Correlation of the PC scores with regional precipitation anomalies reveals an inverse relationship with Florida and Gulf Coast precipitation (Table 3).

The Eastern Pacific teleconnection (Barnston & Livezey 1987) is clearly approximated by the loadings pattern of PC4 (Fig. 3). Component scores relate significantly (Table 3) to High Plains precipitation, indicating that precipitation forcing in the region is related to lower tropospheric heights. The last component (PC5; Fig. 3) represents a pattern which is strongly linked to East Coast precipitation. Lowered heights over west Texas and high heights over the Northeast correspond to positive precipitation anomalies in the region.

4.2.2. Negative Anomaly Months

The primary modes of atmospheric variation present during extreme negative SOI (El Niño) anomaly months (NAM) are shown in Fig. 4. Together, these patterns account for 81% of the dataset variance in the 28 El Niño months. Again, many known teleconnection patterns are readily apparent. It is not surprising that

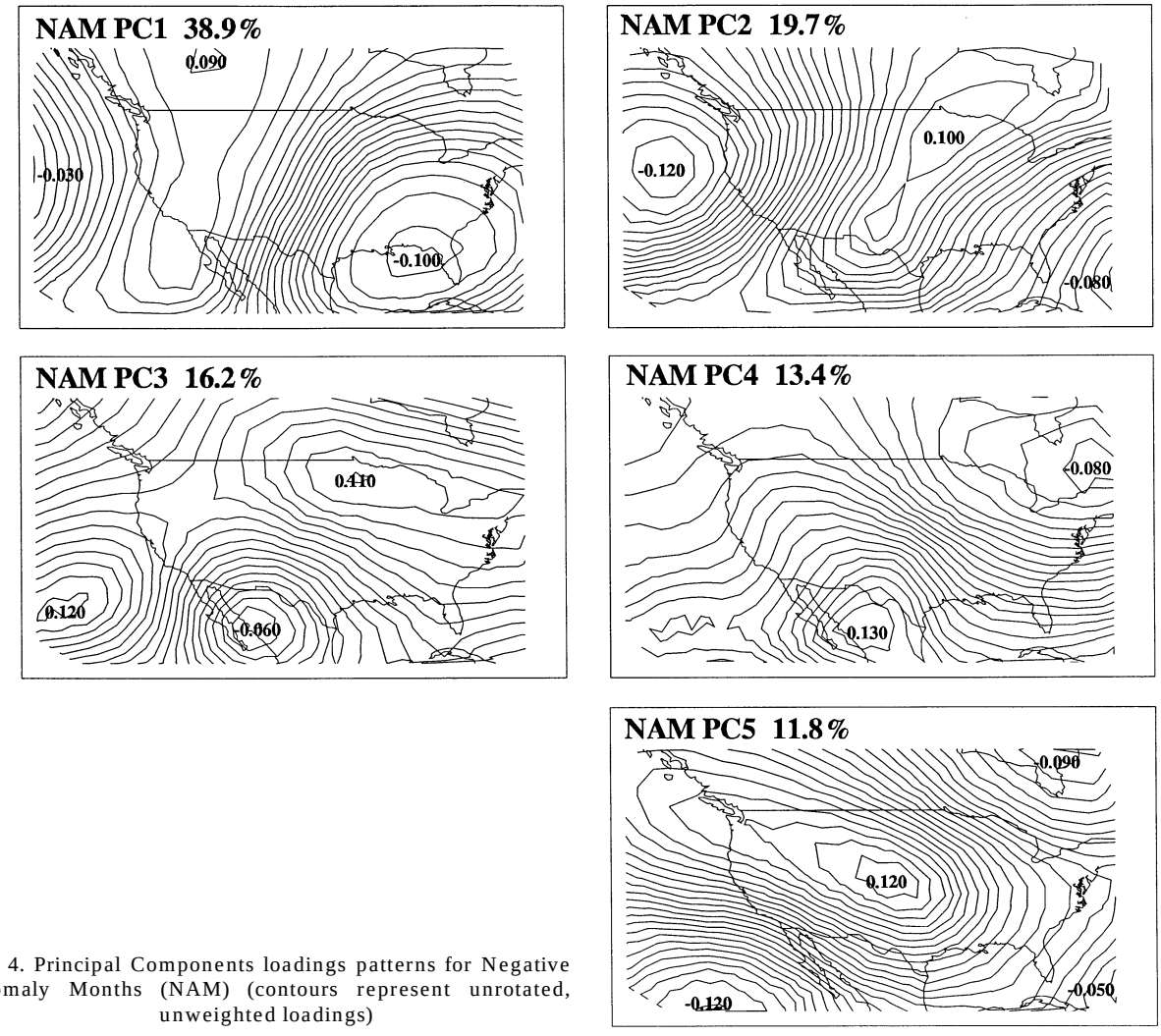

Fig. 4. Principal Components loadings patterns for Negative Anomaly Months (NAM) (contours represent unrotated, unweighted loadings)

the first PC (Fig. 4) is clearly indicative of the PNA pattern during El Niño months. However, somewhat surprisingly is that the pattern is significantly related only to Florida precipitation (Table 4). The weak relationship is in phase with the positive height pattern mode, indicating a similar surface response to lower tropospheric heights as indicated previously.

NAM component 2 (Fig. 4) approximates the TNH pattern. However, unlike the TNH present during the AWM grouping, the pattern proves relatively unimportant to southern U.S. precipitation during El Niño months. PC3 (Fig. 4) appears to be a variation of the ambiguous AWM PC5 pattern. Some differences exist in that during El Niño times the action centers are displaced southwest. The resulting surface relationship is a correlation to Gulf Coast precipitation (Table 4).

PC4 (Fig. 4) is another variant, but has no significant relationship to southern U.S. precipitation. Component 5 (Fig. 4) relates to East Coast precipitation and more strongly to Gulf Coast precipitation (Table 4). Both correlations are negative, indicating that when 500 mb ridging occurs over the western Great Plains, negative precipitation anomalies result in the related regions.

Table 4. Correlations between all NAM PCs and southern United States precipitation regions (abbreviations as in Table 2). Significance ($\alpha = 0.10$) indicated in bold

		PC1	PC2	PC3	PC4	PC5
EC	r	−0.0691	−0.2079	−0.1515	−0.1590	−0.2554
	p	0.6600	0.1810	0.3323	0.3084	**0.0983**
FL	r	0.2689	0.0133	−0.1966	−0.1172	−0.2284
	p	**0.0851**	0.9334	0.2121	0.4598	0.1457
GC	r	0.0311	−0.0648	0.2864	0.0210	−0.4332
	p	0.8449	0.6833	**0.0660**	0.8949	**0.0042**
HP	r	−0.1066	−0.0721	0.1775	0.2028	−0.1440
	p	0.5016	0.6498	0.2607	0.1977	0.3628
NC	r	−0.2049	0.2058	0.0597	0.0562	−0.0575
	p	0.1874	0.1856	0.7040	0.7202	0.7141

4.2.3. Positive Anomaly Months

The primary PAM (positive anomaly month) geopotential height patterns are depicted in Fig. 5. The 5 patterns explain 87% of the variability in monthly heights during the 43 La Niña months. Similarities to known teleconnections are again apparent. However, the first loadings pattern (PC1; Fig. 5) appears to be a hybrid pattern of the PNA and TNH. The in-phase action nodes, over the northeastern North Pacific and Florida, are geographically representative of the PNA pattern while the middle out-of-phase action node is displaced eastward toward Hudson Bay, similar to the displacement evident in the TNH. The pattern relates well to surface precipitation in the southern United States as all 5 regions are significantly negatively correlated (Table 5), suggesting that the positive (negative) pattern mode induces anomalously dry (wet) conditions throughout the entire study region.

PAM component 2 (Fig. 5) shows a dipolar pattern across the United States. In its positive mode the pattern is linked to above normal precipitation departures in the East Coast and North Central regions (Table 5). The positive relationship is difficult to explain given that rising heights over the Midwest induce precipitation in these regions. This PC was the only component which showed a significant change in slope through the scores. The fitted trend-line indicated a significantly positive slope ($r = 0.39$; $p = 0.05$) through the data, indicating significant strengthening of the pattern during recent times.

PC4 (Fig. 5) is the only other PAM component to show a significant relationship to regional precipitation. A weak negative relationship exists between the PC scores and the North Central region (Table 5). The pattern suggests that high (low) heights to the west of the region and low (high) heights to the east are conducive to drier (wetter) than normal conditions.

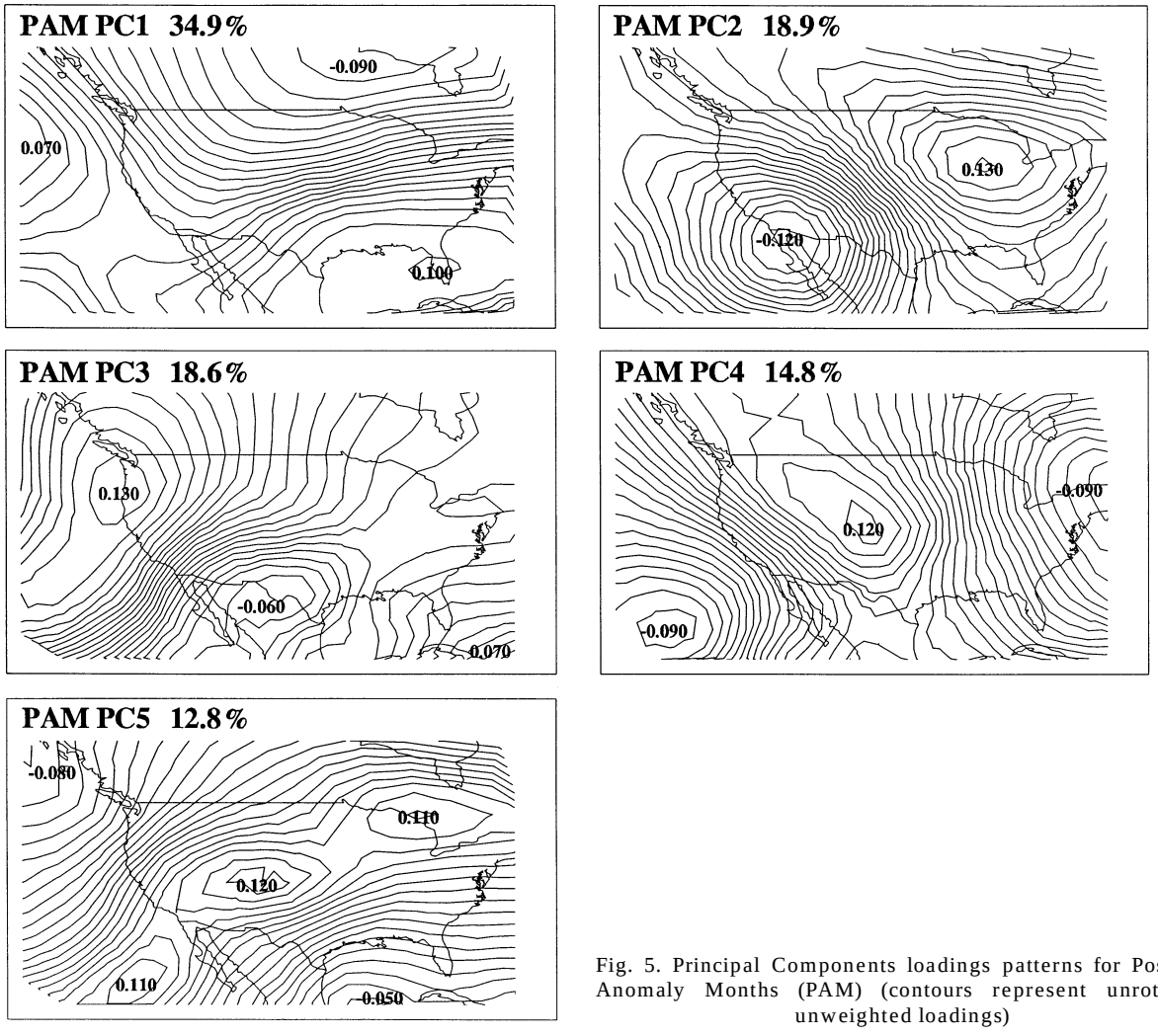

Fig. 5. Principal Components loadings patterns for Positive Anomaly Months (PAM) (contours represent unrotated, unweighted loadings)

Table 5. Correlations between all PAM PCs and southern United States precipitation regions (abbreviations as in Table 2). Significance ($\alpha = 0.10$) indicated in bold

		PC1	PC2	PC3	PC4	PC5
EC	r	−0.3594	0.4233	−0.2776	−0.2266	0.0228
	p	**0.0846**	**0.0393**	0.1891	0.2870	0.9157
FL	r	−0.6207	0.0509	−0.0720	−0.0199	0.2213
	p	**0.0012**	0.8130	0.7383	0.9266	0.2988
GC	p	−0.4656	0.2716	−0.1952	−0.1988	0.2255
	r	**0.0219**	0.1992	0.3608	0.3518	0.2894
HP	r	−0.4459	0.2333	−0.2428	−0.2698	0.1679
	p	**0.0290**	0.2726	0.2529	0.2023	0.4327
NC	r	−0.3468	0.3664	−0.3363	−0.3463	0.0793
	p	**0.0969**	**0.0782**	0.1081	**0.0973**	0.7126

5. DISCUSSION AND CONCLUSIONS

This research analyzed the mid-tropospheric response between extreme phases of the SOI. Gridded 500 mb geopotential heights over the conterminous U.S. were extracted for both negative and positive anomaly months (NAM and PAM, respectively) of the Southern Oscillation Index. The data were subjected to Principal Components Analysis and primary patterns derived. Further comparisons were made to a baseline climatology of mid-tropospheric height variations during all cool season (November to March) months (AWM). Correlations between the principal component scores and regional precipitation anomalies determined the relationship of the derived patterns to the surface environment.

Correlation results suggest that a cool season precipitation response in the southern United States is driven, at least in part, by phases of the SOI. In general, the positive SOI phase (La Niña) elicits a greater surface response than its negative (El Niño) counterpart. Analysis suggests that the primary longwave flow variations change depending on SOI phase as compared to the base climatology of mid-tropospheric heights. Also, variability is high within the extreme phases of the SOI, indicating that individual El Niño and La Niña winters are rarely similar with regard to atmospheric flow.

During NAMs, the resulting 500 mb patterns approximate those exhibited during AWMs. The patterns drive similar precipitation forcing as well. This suggests that during El Niño years there is quite a variation of circulation patterns (Fig. 4); however, the PNA seems to be most important. During PNA flow regimes, the greatest surface response occurs in Florida. During positive PNA flow regimes, Florida underlies a region of positive vorticity advection associated with displaced jet troughing over the northern Gulf Coast. This provides adequate venting through the mid- to upper-troposphere (Hsu 1993), inducing both a higher frequency of mid-latitude cyclones (Manty 1993) and heavier magnitude precipitation events throughout the southern U.S. (Keim 1997). Such an alignment in the 500 mb height field also relates well to meteorological 'bombs' which are more common in this area during El Niño times (Hsu 1993). Positive precipitation departures result in the Florida peninsula. More northerly regions are embedded in cool dry air associated with migratory anticyclones extending from Canada (Rogers & Rohli 1991). This results in negative or near zero precipitation departures in those regions. During negative PNA phases, near zonal or reverse (a longwave trough over the Rockies and ridging over the eastern Pacific and eastern U.S.) flow dominates, causing an inverse surface response as the more northerly regions are in the area of greatest positive vorticity advection and wave cyclone passage (Bierly & Harrington 1995) while the southerly regions lie in a region of high heights and limited precipitation forcing.

Similar variations occur during AWMs, suggesting that during El Niño months both zonal and meridional flow regimes are important. Therefore, the PNA has little influence outside of Florida during El Niño times because whether the longwave flow is zonal or meridional, the enhanced jet, induced by lower heights over the Gulf of Mexico, advects copious moisture regardless of Rossby Wave variability.

During La Niña (PAM) winters different patterns seem to control precipitation variability. During these times, the most important geopotential height configuration is a hybrid pattern between the PNA and TNH teleconnections. The pattern exhibits eastward-displaced Northern Pacific and (especially) Cordillera action nodes. Such displacement represents the most dramatic changes between the phases of the SOI examined and the derived base climatology and suggests that a true PNA pattern is not typically forced by extreme positive SOI departures. The geographic alignment of the southeastern U.S. action center approximates that of the PNA, which suggests that height variations over the northwestern Pacific and Gulf of Mexico are still most important to southern U.S. precipitation during PAMs. Variations over the Gulf of Mexico strongly influence jet strength over the region (Manty 1993). When heights over the area are high (low), the jet is weak (strong) which induces negative (positive) precipitation departures in all regions through a reduction in cyclonic activity. It is speculated that the height variability is driven, at least in part, by more frequent migrations of polar anticyclones during La Niña times. Future studies should further detail the relationships between La Niña forcing and geopotential height variability as they relate to anticyclone migrations over the southern U.S.

Appendix 1. Eigenvalues of the correlation matrix for all AWM, PAM and NAM unrotated principal components

	Eigenvalue	Difference	Proportion	Cumulative
(a) All Winter Months				
PC1	76.462	37.682	0.315	0.315
PC2	38.779	6.959	0.159	0.474
PC3	31.821	5.659	0.131	0.605
PC4	26.162	2.958	0.108	0.713
PC5	23.204	6.842	0.095	0.808
PC6	16.363	9.446	0.067	0.876
PC7	6.916	0.418	0.028	0.904
PC8	6.498	1.496	0.027	0.931
(b) Positive Anomaly Months				
PC1	73.511	33.400	0.303	0.303
PC2	40.110	0.852	0.165	0.468
PC3	39.259	7.940	0.162	0.629
PC4	31.319	4.247	0.129	0.758
PC5	27.071	18.944	0.111	0.869
PC6	8.127	1.806	0.033	0.903
PC7	6.320	1.401	0.026	0.949
PC8	4.919	0.623	0.020	0.966
(c) Negative Anomaly Months				
PC1	76.462	37.682	0.315	0.315
PC2	38.779	6.959	0.159	0.474
PC3	31.821	5.659	0.131	0.605
PC4	26.162	2.958	0.108	0.713
PC5	23.204	6.842	0.095	0.808
PC6	16.363	9.446	0.067	0.876
PC7	6.916	0.418	0.028	0.904
PC8	6.498	1.496	0.027	0.931

Acknowledgements. The authors thank Dr Brent Yarnal and the anonymous reviewers for their contributions to the manuscript. We also thank Jeff Duncan for his assistance with the figures. This work was funded through the NASA JOVE (JOint VEnture) Research Alliance.

LITERATURE CITED

Angel JK, Korshover J (1987) Variability in United States cloudiness and the relation to El Niño. J Clim Appl Meteorol 26(5):580–584

Arkin PA, Chen WY, Rasmusson EM (1980) Fluctuations in mid and upper tropospheric flow associated with the Southern Oscillation. Proc 5th Ann Clim Diag Workshop. US Dept of Commerce, Washington, DC

Barnston AG, Livezey RE (1987) Classification, seasonality and persistence of low-frequency atmospheric circulation patterns. Mon Wea Rev 115:1083–1126

Bierly GD, Harrington JA Jr (1995) A climatology of transition season Colorado cyclones: 1961–1990. J Clim 8: 853–863

Bjerknes J (1969) Atmospheric teleconnections from the equatorial Pacific. Mon Wea Rev 97(3):163–172

Bradley RS, Diaz JF, Kiladis GN, Eischeid JK (1987) ENSO signal in continental temperature and precipitation record. Nature 327:497–501

Buell CE (1975) The topography of the empirical orthogonal functions. Preprints, Fourth Conference on Probability and Statistics in Atmospheric Sciences, Tallahassee, FL. American Meteorological Society, Boston, MA, p 188–193

Conrad V (1941) The variability of precipitation. Mon Wea Rev 69:5–11

Dickson RR, Namias J (1976) North American influences on the circulation and climate of the North Atlantic sector. Mon Wea Rev 104:1255–1265

Douglas AV, Englehart PJ (1981) On a statistical relationship between autumn rainfall in the central equatorial Pacific and subsequent winter precipitation in Florida. Mon Wea Rev 190:2377–2382

Dunteman GH (1989) Principal components analysis. Sage University Paper series on Quantitative Applications in the Social Sciences, 07-069. Sage Publ, Beverly Hills

Henderson KG, Vega AJ (1996) Regional precipitation variability in the southern United States. Phys Geogr 17(2): 93–112

Hsu SA (1993) The Gulf of Mexico—a breeding ground of winter storms. Mariners Wea Log, Spring, p 4–7, 10–11

Keim BD (1997) Preliminary analysis of the temporal patterns of heavy rainfall across the southeastern United States. Prof Geog 49:1:94–104

Leathers DJ, Yarnal B, Palecki MA (1991) The Pacific/North American teleconnection pattern and the United States climate. Part I: Regional temperature and precipitation associations. J Clim 4:517–528

Lewis JK, Hsu SA (1992) Mesoscale air-sea interactions related to tropical and extratropical storms in the Gulf of Mexico. J Geophys Res 97(C2):2215–2228

MacDonald BC, Reiter EA (1988) Explosive cyclogenesis over the eastern United States. Mon Wea Rev 116: 1568–1586

Manty RE (1993) Effect of the El Niño/Southern Oscillation on Gulf of Mexico, winter, frontal-wave cyclones: 1960–89. PhD dissertation, Louisiana State University, Baton Rouge

Mo KC, Livezey RE (1986) Tropical-extratropical geopotential height teleconnections during the Northern Hemisphere winter. Mon Wea Rev 114:2488–2515

NCAR (1993) Compact disc of the National Meteorological Center Grid Point Data Set: Version II. Department of Atmospheric Sciences, University of Washington, Seattle, WA; and Data Support Section, National Center for Atmospheric Research, Boulder, CO

Nicholls N (1988) ENSO and rainfall variability. J Clim 1(4): 418–421

Philander SG (1990) El Niño, La Niña, and the Southern Oscillation. Academic Press, San Diego

Rasmusson EM, Carpenter TH (1982) Variations in tropical sea surface temperatures and surface wind fields associated with the Southern Oscillation/El Niño. Mon Wea Rev 110:354–384

Rogers JC, Rohli RV (1991) Florida citrus freezes and polar anticyclones in the Great Plains. J Clim 4:1103–1113

Ropelewski CF, Halpert MS (1987) Global and regional scale precipitation patterns associated with ENSO. Mon Wea Rev 115:1606–1626

Sanders F, Gyakum JR (1980) Synoptic-dynamic climatology of the 'bomb'. Mon Wea Rev 108:1589–1606

Trenberth KE (1976) Spatial and temporal variations in the Southern Oscillation. Q J R Meteorol Soc 102:639–653

Vega AJ, Sui CH, Lau KM (1997) Northern Hemisphere flow anomalies and US temperature and precipitation variability. Proceedings of the 1997 Applied Geography Conference. Applied Geography Conferences, Inc, 20: 204–209

Walker ND (1993) A preliminary look at cyclogenesis in the Gulf of Mexico during the March 1993 blizzard. Mariners Wea Log, Spring, p 8–9

Wallace JM, Gutzler DS (1981) Teleconnections in the geopotential height field during the Northern Hemisphere winter. Mon Wea Rev 109:784–812

Yarnal B (1993) Synoptic climatology in environmental analysis — a primer. Belhaven Press, London

Yarnal B, Leathers DJ (1988) Relationships between interdecadal and interannual climatic variations and their effect on Pennsylvania climate. Annls Assoc Am Geog 78(4):624–641

Editorial responsibility: Brent Yarnal, University Park, Pennsylvania, USA

Submitted: October 4, 1996; Accepted: June 10, 1998
Proofs received from author(s): June 26, 1998